
Development and Implementation of Symmetry-adaptation techniques for Quantum Dynamics in large systems

By Xiaohu Li

Advisor: Srinivasan S. Iyengar

I. Introduction

In chemical reactions, most of the nuclei can be considered as classical particles, and dynamics using classical methods successfully describe the process of chemical reaction. The electrons do need to be treated quantum-mechanically to understand chemical reactions. But in some reactions, the behavior of some nuclei is quantum mechanical; the classical method is not accurate anymore. The main difference between classical mechanics and quantum mechanics is that in

quantum mechanics, particles need to be treated as wave function on account of the DeBroglie wave/particle duality. For example, hydrogen bonding properties involving protons can be affected by nuclear quantization. Studying the behavior of the proton will help us understand the mechanism of some reaction, where proton transfer plays an important role. Hence, there is a need to study these problems using Quantum Dynamics.

II. Review of background in my research

2.1 Quantum Wave packet Atom-centered Density Matrix Propagation

Recently, a quantum dynamics approach—Atom-centered Density Matrix Propagation (ADMP) has been developed, which is used to treat electron-nuclear dynamics in large systems. The method turns out to be very powerful. In this scheme, the electronic structure, represented using the single particle electronic density matrix, is propagated simultaneously with the classical nuclei by a simple adjustment of the relative nuclear and electronic time-scales, which is effected by using an extended Lagrangian scheme. In other words, in ADMP, both the nuclei and electrons are treated by classical method, but in some systems, certain subsystems behave quantum mechanically, so instead of applying ADMP on this subsystem, we will use Quantum Wave packet Propagation, which basically treat s the subsystem as wave function and let the wave function propagate in the space. The method to treat the whole systems is called Quantum Wave packet Atom-centered Density Matrix Propagation. The Quantum Wave packet Propagation can also be combined with Born-Oppenheimer dynamics to study a large system, in

which the nuclei and electrons are treated using BO, and the quantum subsystem is treated using Quantum Wave packet Propagation.

The main steps for the Quantum Wave packet ADMP propagation is as follows: First we start from the fundamental equation in quantum mechanics—the Time-Dependent Schrödinger Equation (TDSE).

$$i\hbar \frac{\partial}{\partial t} \psi(r, R; t) = H\psi(r, R; t) \quad (1)$$

If we assume that these individual parts of the full system only interact with each other in an average sense then we may employ Dirac's Time-Dependent Self-Consistent Field (TDSCF) method like partitioning scheme where the full electron-nuclear system is divided into three parts: subsystem 1 will be treated quantum dynamically, subsystem 2 and subsystem 3 will be treated using ADMP or BO. Based on TDSCF, we can reduce Eq. (1) into three separate equations

$$i\hbar \frac{\partial}{\partial t} \psi_1(R_{QM}; t) = H_1\psi_1(R_{QM}; t) \quad (2)$$

$$i\hbar \frac{\partial}{\partial t} \psi_2(R_C; t) = H_2\psi_2(R_C; t) \quad (3)$$

$$i\hbar \frac{\partial}{\partial t} \psi_3(r, t) = H_3\psi_3(r, t) \quad (4)$$

Eq. (3) and Eq. (4) stand for classical nuclei and electrons; they will be treated using ADMP.

For Eq. (2), the solution is $\psi(t + \Delta t) = \exp\left\{-i\hat{H}t/\hbar\right\}\psi(t)$, where

$\exp\left\{-i\hat{H}t/\hbar\right\}$ is called propagator. It propagates the wave function from time =

t to time = t + Δt . If we guess the initial wave packet of the quantum mechanical

system at time = 0, then by using the propagator, we can obtain the wave function at any time. Thus, any observable physical property can be obtained using the wave function. Symbol \hat{H} is the Hamiltonian operator, which is a sum of kinetic ($\hat{\kappa}$) operator and potential (\hat{v}) energy operator.

2.2 Distributed Approximating Functional for kinetic propagator

The propagator can be approximated using a kinetic reference symmetric split operator approach:

$$\exp\left\{-i\hat{H}\Delta t/\hbar\right\} = \exp\{-i\hat{v}\Delta t/2\hbar\}\exp\{-i\hat{\kappa}\Delta t/\hbar\}\exp\{-i\hat{\kappa}\Delta t/2\hbar\} + o(\Delta t^3) \quad (5)$$

We use this approximation because it provides dynamics that strictly obeys time-reversal symmetry. In the position representation, the potential energy operator is local. Numerically, this means the matrix for the potential part $\exp\{-i\hat{\kappa}\Delta t/2\hbar\}$ is diagonal. The free propagator is local in momentum representation, but non-local in position representation, which means the matrix, is not diagonal anymore. There are several approaches to obtain the result of free propagator acting on wave packet. In current work, we use Distributed Approximating Functional (DAF) representation for the position representation of the free propagator. In this representation, the free propagator is a banded, sparse matrix.

III. Research Work

3.1 A brief view of my research

The quantum mechanical subsystem we are going to study is actually a quantum particle in potential well. The particle is confined to the potential well, which in turn, is created by the movement of the surrounding classical atoms and electrons. For given classical nuclei geometry and density matrix, move the quantum along the uniform grid point, on every grid point, solve the Time-Independent Schrödinger Equation for the quantum particle, we can get the potential energy surface along the grid space. In ADMP, the potential energy is written as a density functional using McWeeny purification for the density matrix. For this particle in a box problem, the wave function is zero on and outside the boundaries. This is the boundary condition for solving Eq. (2), which is called Dirichlet boundary condition. The construction of DAF representation for free propagator at the grid point needs the information of wave function from the locus of points close to it. So near the boundaries, the results using the DAF representation for free propagator is not as accurate as in the middle of the potential well, because we don't have wave function outside the box. Thus, a more stable representation for free propagator is needed.

3.2 Symmetry-adapted DAF Representation for free propagator

3.2.1 DAF Representation for free propagator

$$\begin{aligned}
\langle R_{QM} | \exp \left\{ -\frac{iK\Delta t_{QM}}{\hbar} \right\} | R'_{QM} \rangle_{DAF} &= \frac{1}{\sigma(0)} \exp \left\{ -\frac{(R_{QM} - R'_{QM})^2}{2\sigma(\Delta t_{QM})^2} \right\} \times \\
\sum_{n=0}^{M/2} \left(\frac{\sigma(0)}{\sigma(\Delta t_{QM})} \right)^{2n+1} \left(\frac{-1}{4} \right)^n \frac{1}{n!} (2\pi)^{-1/2} \times & \\
H_{2n} \left(\frac{R_{QM} - R'_{QM}}{\sqrt{2}\sigma(\Delta t_{QM})} \right) &
\end{aligned} \tag{6}$$

Where

$$\left\{ \sigma(\Delta t_{QM}) \right\}^2 = \sigma(0)^2 + \frac{i\Delta t_{QM} \hbar}{M_{QM}} \tag{7}$$

And $H_{2n}(x)$ are Hermite polynomials of even order. Eq. (6) is obtained from the well-known analytical expression for free evolution of a Gaussian function,

$$\begin{aligned}
&\exp \left\{ -\frac{iK\Delta t_{QM}}{\hbar} \right\} \exp \left[-\frac{x^2}{2\sigma(0)^2} \right] \\
&= \frac{\sigma(0)}{\sigma(\Delta t_{QM})} \exp \left[-\frac{x^2}{2\sigma(\Delta t_{QM})^2} \right]
\end{aligned} \tag{8}$$

along with the fact that the Hermite functions are generated from Gaussians according to

$$H_n(x) \exp \left[-\frac{x^2}{2\sigma^2} \right] = (-1)^n \frac{d^n y}{dx^n} \exp \left[-\frac{x^2}{2\sigma^2} \right] \tag{9}$$

Since the derivative operators $\frac{d^n}{dx^n}$ commute with the free propagator, the Hermite functions can be used as a basis to expand the exact quantum free propagator with coefficients as described in Eq. (6). This yields an efficient propagation scheme to perform quantum dynamics and Feynman path integration

through the action of a banded, sparse, Toeplitz matrix on a vector.

Eq. (6) is presented in its continuous form and is valid for all values of R_{QM} and R'_{QM} . Here the free evolution of a wave packet $\chi(R_{QM};t)$ is obtained by discretization:

$$\begin{aligned} & \chi(R_{QM};t + \Delta t) \\ &= \int dR'_{QM} \langle R_{QM} | \exp\left\{-\frac{iK\Delta t_{QM}}{\hbar}\right\} | R'_{QM} \rangle_{DAF} \chi(R'_{QM};t) \end{aligned} \quad (10)$$

It is also noted that,

$$\lim_{\Delta t \rightarrow 0} \langle R_{QM} | \exp\left\{-\frac{iK\Delta t_{QM}}{\hbar}\right\} | R'_{QM} \rangle \equiv \delta(R_{QM} - R'_{QM}) \quad (11)$$

For DAF approximation, this become true only at large values of M,

$$\lim_{\Delta t \rightarrow 0} \langle R_{QM} | \exp\left\{-\frac{iK\Delta t_{QM}}{\hbar}\right\} | R'_{QM} \rangle_{DAF} \equiv \delta_{DAF}(R_{QM} - R'_{QM}) \approx \delta(R_{QM} - R'_{QM}) \quad (12)$$

$$\begin{aligned} & \chi(R'_{QM};t + \Delta t) \\ &= \frac{\Delta x}{\sigma(0)} \sum_j \exp\left\{-\frac{(R'_{QM} - R^j_{QM})^2}{2\sigma(\Delta t_{QM})^2}\right\} \sum_{n=0}^{M/2} \left(\frac{\sigma(0)}{\sigma(\Delta t_{QM})}\right)^{2n+1} \\ & \times \left(\frac{-1}{4}\right)^n \frac{1}{n!} (2\pi)^{-1/2} \times H_{2n}\left(-\frac{R'_{QM} - R^j_{QM}}{\sqrt{2}\sigma(\Delta t_{QM})}\right) \chi(R^j_{QM};t) \end{aligned} \quad (13)$$

Where Δx is the grid discretization in one dimension. The variables M and $\sigma(0)$ determine the accuracy and width of the DAF. These parameters are not independent and for a given value of M there exists a $\sigma(0)$ that provides optimal accuracy for the propagation.

3.2.2 Construction of Symmetry-adapted DAF Representation for free propagator

As we discussed, the wave function for the quantum particle is not continuous

on the boundaries, the wave function on and outside the boundaries is zero and the propagation does not work very well near the boundaries. The approach to overcome this shortage is to assume that we have wave function in the whole space, and the wave function has some symmetry properties. The simplest symmetry a one dimensional wave function can have in space is C_{2v} . For example, our wave function inside the potential well looks like:

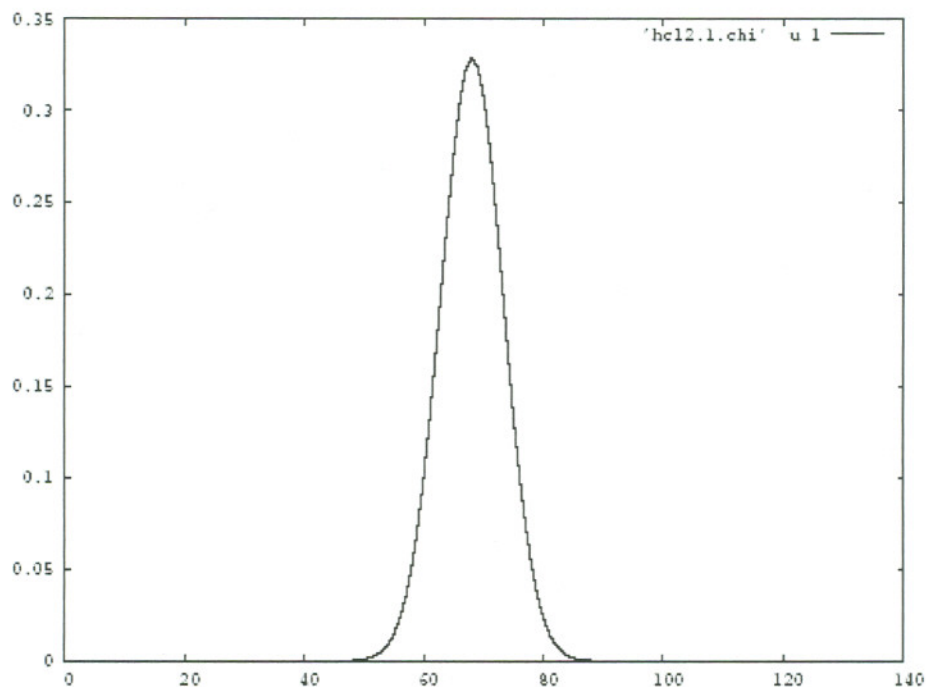


Figure 1 Wave function in potential well

After expanding the wave function in the whole space and make it have C_{2v} symmetry, the wave function looks like:

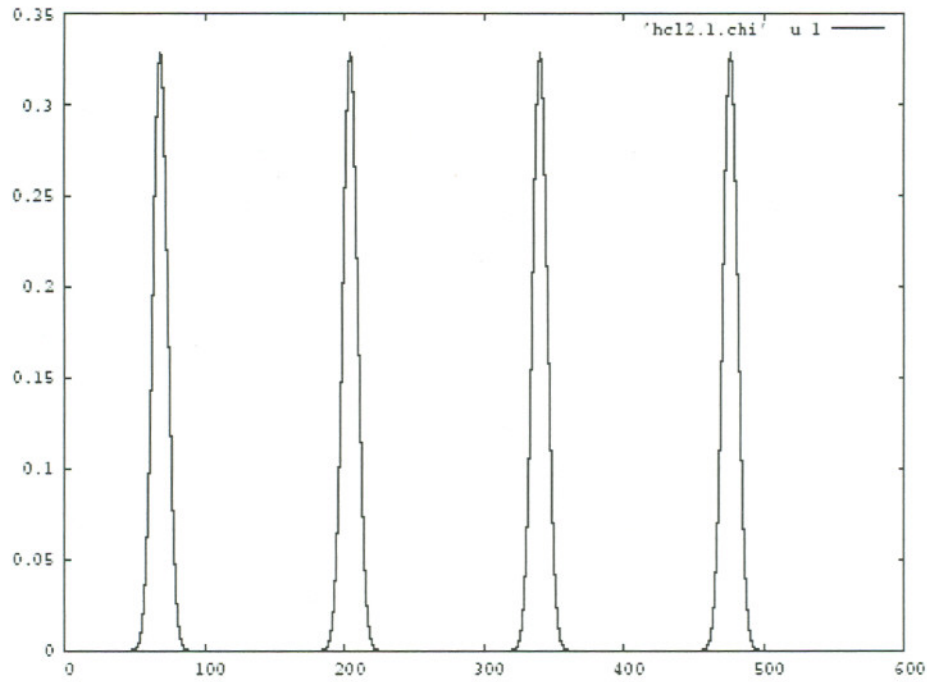


Figure 2 Expanded Wave function in whole space

We can see that after expansion, the wave function is continuous in the whole space. The first derivative is zero on the boundaries, which is called Neumann boundary condition for differential equation.

Eq. (10) can be written as,

$$\begin{aligned} & \chi(R_{QM}; t + \Delta t) \\ &= \int_{-\infty}^{+\infty} dR'_{QM} \delta_{DAF}(R_{QM} - R'_{QM}) \chi(R'_{QM}; t) \end{aligned} \quad (14)$$

Where $\delta_{DAF}(R_{QM} - R'_{QM})$ is the DAF representation for free propagator. After expansion, the wave function becomes periodic with period of four times of the length of the box L . Eq. (11) is simplified to,

$$\begin{aligned} & \chi(R_{QM}; t + \Delta t) \\ &= \int_0^{4L} dR'_{QM} D_{DAF}(R_{QM} - R'_{QM}) \chi(R'_{QM}; t) \end{aligned} \quad (15)$$

Where $D_{DAF}(R_{QM} - R'_{QM}) = \sum_{n=-\infty}^{+\infty} \delta_{DAF}(R_{QM} - R'_{QM} + 4nL)$. Although we take the limit of sum to be infinite, the banded nature of $\delta_{DAF}(R_{QM} - R'_{QM})$ assures that the DAF is significantly nonzero only in a finite neighborhood of R_{QM} . Hence, the upper and lower limits of the sum can be taken, in fact, to be finite and small. The actual values chosen, however, depend on the choice of σ/Δ (here, Δ is the grid spacing between uniform grid points) and M (for the Hermite-DAF), and the number of grid points, N . Hence,

$D_{DAF}(R_{QM} - R'_{QM}) = \sum_{n=-n_0}^{n_0} \delta_{DAF}(R_{QM} - R'_{QM} + 4nL)$ is a numerically accurate definition.

We now further reduce $D_{DAF}(R_{QM} - R'_{QM})$ operator, using C_{2v} symmetry. We have seen that after expansion of the wave function, it has C_{2v} symmetry in the interval $[0, 4L]$. So Eq. (12) can be simplified further to,

$$\begin{aligned} & \chi(R_{QM}; t + \Delta t) \\ &= \int_0^L dR'_{QM} \bar{T}_{DAF}(R_{QM}, R'_{QM}) \chi(R'_{QM}; t) \end{aligned} \quad (16)$$

Here, $T_{DAF}(R_{QM}, R'_{QM})$ is the symmetry-adapted representation for the free propagator, it contains all the symmetry information of the wave function belonging to C_{2v} group.

The wave function now have some symmetry belongs to C_{2v} group. The C_{2v} character table has the following form,

C_{2v}	E	C_2 (z)	$\sigma_v(xz)$	$\sigma_v(yz)$	linear functions, rotations	quadratic functions	Cubic functions
A_1	+1	+1	+1	+1	z	x^2, y^2, z^2	z^3, x^2z, y^2z
A_2	+1	+1	-1	-1	R_z	xy	χyz
B_1	+1	-1	+1	-1	x, R_y	xz	xz^2, x^3, xy^2
B_2	+1	-1	-1	+1	y, R_x	yz	yz^2, y^3, x^2y

It is obvious that our expanded wave function has A_1 symmetry, and hence we can use the character of A_1 symmetry and the “Great Orthogonality Theorem” to construct the symmetry-adapted DAF representation for free propagator as:

$$\begin{aligned}
 & T_{DAF}(R_{QM}^i, R_{QM}^j) \\
 &= \frac{\sqrt{2 - \delta_{R_{QM}^i, 0} - \delta_{R_{QM}^j, \pi/2}}}{\sqrt{2}} \left[D_{DAF}(R_{QM}^i - R_{QM}^j) + \right. \\
 & D_{DAF}(R_{QM}^i - R_{QM}^j - 2L) + D_{DAF}(R_{QM}^i + R_{QM}^j) \\
 & \left. + D_{DAF}(R_{QM}^i + R_{QM}^j - 2L) \right] \frac{\sqrt{2 - \delta_{R_{QM}^i, 0} - \delta_{R_{QM}^j, \pi/2}}}{\sqrt{2}}
 \end{aligned} \tag{17}$$

$\frac{\sqrt{2 - \delta_{R'_{QM},0} - \delta_{R'_{QM},\pi/2}}}{\sqrt{2}}$ and $\frac{\sqrt{2 - \delta_{R'_{QM},0} - \delta_{R'_{QM},\pi/2}}}{\sqrt{2}}$ are the factors due to the trapezoid-rule quadrature approximation to the integral in Eq. (13) using grid points $\{R'_{QM}\}$.

The expression of the symmetry-adapted DAF representation is written to code using FORTRAN 77, and numerical test is done based on the a Gaussian-like wave function (see Appendix).

IV Result

4.1 The comparison of propagation between the non-symmetry-adapted and symmetry-adapted DAF for free propagator

The parameters are chosen as follows:

$M_{QM} = 1837.15265$ a.u, $\Delta t = 0.413437$ a.u, the grid spacing $\Delta R_{QM} = 0.3149533$ a.u, number of grid points is 137

First, we compare the $|(\psi^i_{non-symmetry} - \psi^i_{symmetry})|$ at every uniform grid point, where $\psi^i_{non-symmetry}$ means the propagated wave function with non-symmetry adapted DAF, $\psi^i_{symmetry}$ is the propagated wave function with symmetry adapted DAF. We also get the standard deviation,

$$\sigma = \frac{\sqrt{\sum_{i=1}^N |(\psi^i_{non-symmetry} - \psi^i_{symmetry})|^2}}{N} \quad (18)$$

Where N is the number of grid points.

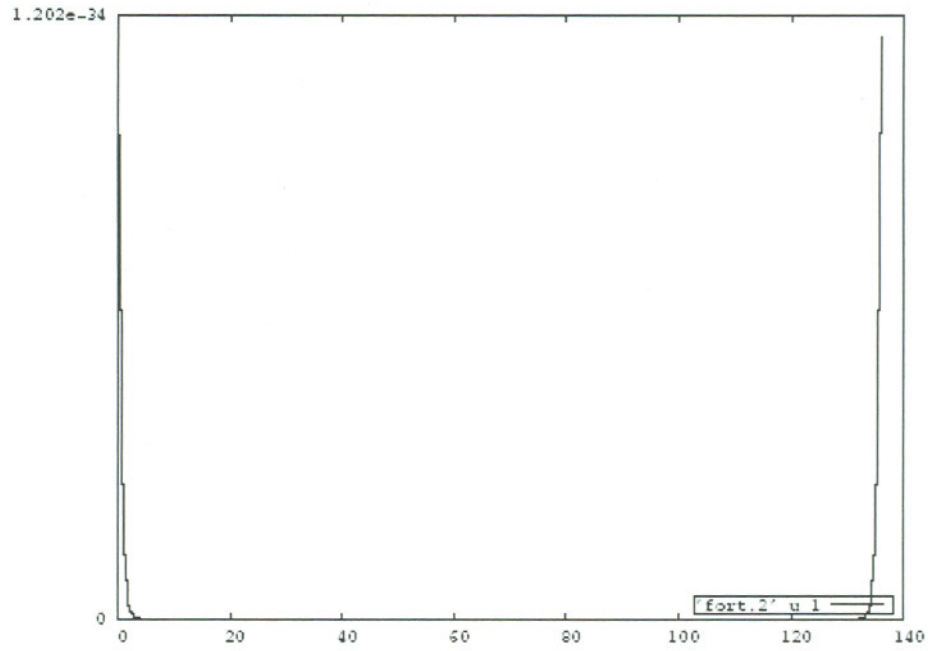


Figure 3 Deviation between the non-symmetry adapted and symmetry adapted DAF when $M=20$

The standard deviation is 1.2068×10^{-36} when $M=20$

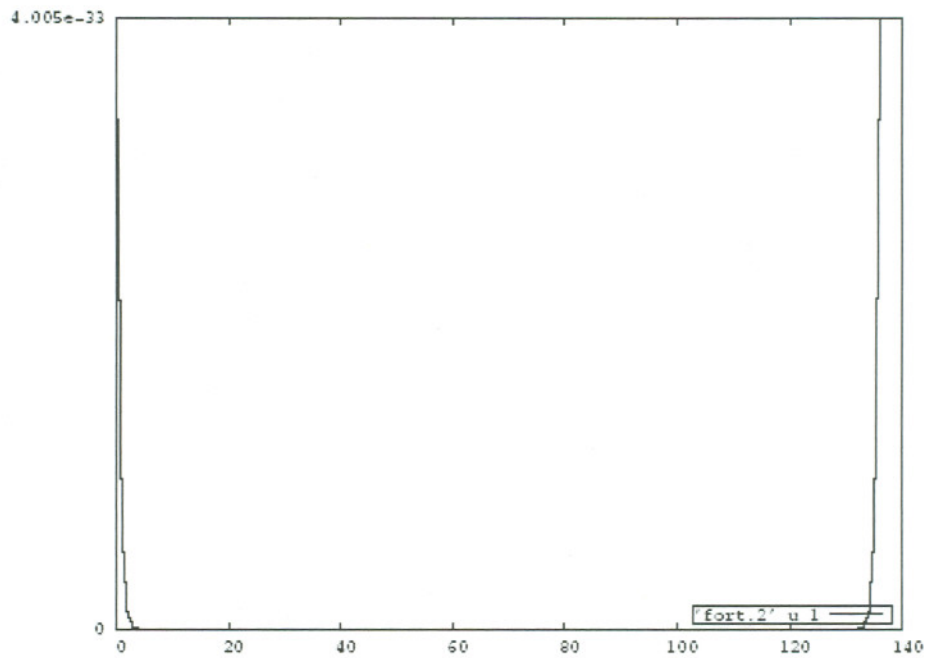


Figure 4 Deviation between the non-symmetry adapted and symmetry adapted DAF when $M=30$

The standard deviation is 4.1678×10^{-35} for $M=30$

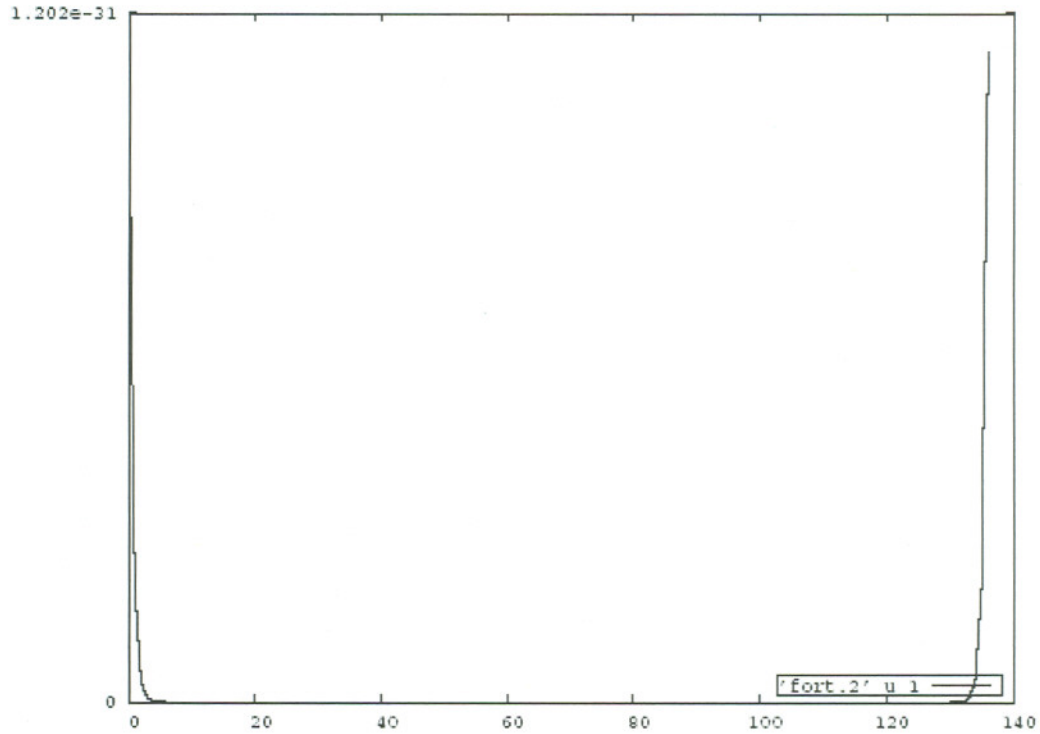


Figure 5 Deviation between the non-symmetry adapted and symmetry adapted DAF when $M=40$

The standard deviation is 1.1889×10^{-33} for $M=40$

So we can see that the symmetry-adapted DAF is a good approximation for the free propagator.

4.2 The test for $\Delta t \rightarrow 0$ of symmetry-adapted DAF

We let $\Delta t = 0$, then as we said before, the DAF is a good approximation of Dirac function.

We compare the original function and the function with,

$$\begin{aligned} & \chi(R_{QM}; t) \\ &= \int_0^L dR'_{QM} \delta_{DAF}(R_{QM}, R'_{QM}) \chi(R'_{QM}; t) \end{aligned} \quad (19)$$

We choose $M=20$, plot $|\chi(R_{QM}; t) - \chi(R'_{QM}; t)|$

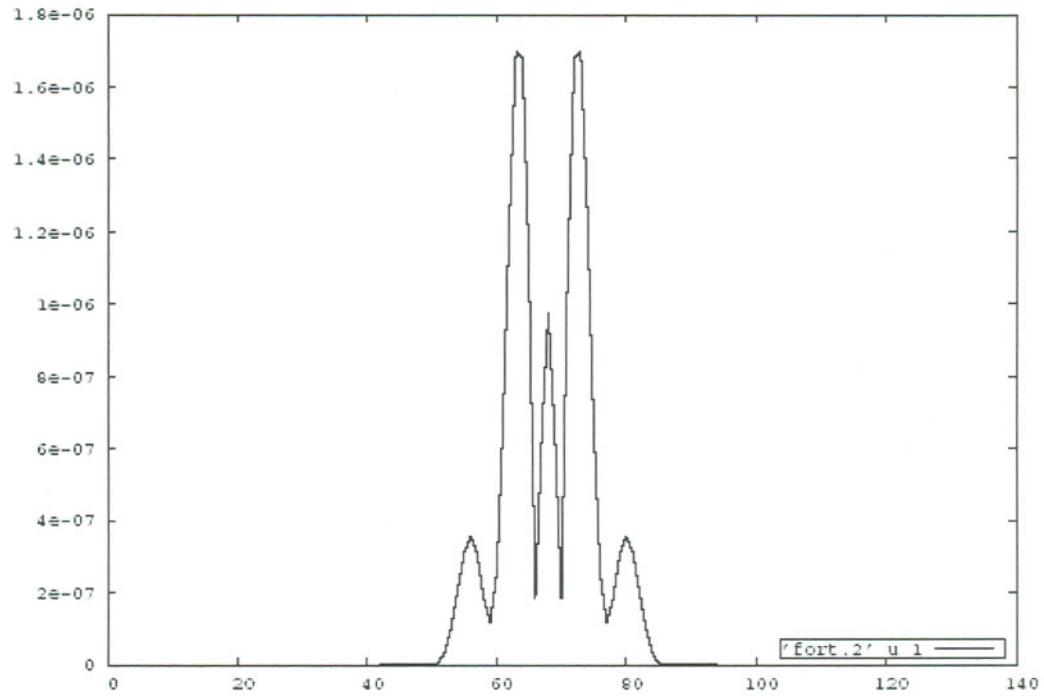


Figure 6 The deviation between the original function and the new function

So we can see that the DAF is a good approximation to Dirac function.

.V Future work

My future work is to put my symmetry-adapted code in Gaussian, and do dynamics research of MMO.

.VI Appendix

0.3352E-37 0.0000E+00

0.4030E-36 0.0000E+00

0.4670E-35 0.0000E+00

0.5216E-34 0.0000E+00

0.5614E-33 0.0000E+00

0.5825E-32 0.0000E+00

0.5825E-31 0.0000E+00

0.5614E-30 0.0000E+00

0.5216E-29 0.0000E+00

0.4670E-28 0.0000E+00
0.4030E-27 0.0000E+00
0.3352E-26 0.0000E+00
0.2687E-25 0.0000E+00
0.2076E-24 0.0000E+00
0.1546E-23 0.0000E+00\
0.1110E-22 0.0000E+00
0.7679E-22 0.0000E+00
0.5120E-21 0.0000E+00
0.3291E-20 0.0000E+00
0.2038E-19 0.0000E+00
0.1217E-18 0.0000E+00
0.7003E-18 0.0000E+00
0.3884E-17 0.0000E+00
0.2076E-16 0.0000E+00
0.1070E-15 0.0000E+00
0.5312E-15 0.0000E+00
0.2543E-14 0.0000E+00
0.1173E-13 0.0000E+00
0.5216E-13 0.0000E+00
0.2235E-12 0.0000E+00
0.9232E-12 0.0000E+00
0.3675E-11 0.0000E+00
0.1410E-10 0.0000E+00
0.5216E-10 0.0000E+00
0.1859E-09 0.0000E+00
0.6387E-09 0.0000E+00
0.2115E-08 0.0000E+00
0.6750E-08 0.0000E+00
0.2076E-07 0.0000E+00
0.6156E-07 0.0000E+00

0.1759E-06 0.0000E+00
0.4845E-06 0.0000E+00
0.1286E-05 0.0000E+00
0.3291E-05 0.0000E+00
0.8115E-05 0.0000E+00
0.1929E-04 0.0000E+00
0.4419E-04 0.0000E+00
0.9757E-04 0.0000E+00
0.2076E-03 0.0000E+00
0.4259E-03 0.0000E+00
0.8420E-03 0.0000E+00
0.1604E-02 0.0000E+00
0.2946E-02 0.0000E+00
0.5216E-02 0.0000E+00
0.8898E-02 0.0000E+00
0.1463E-01 0.0000E+00
0.2319E-01 0.0000E+00
0.3542E-01 0.0000E+00
0.5216E-01 0.0000E+00
0.7401E-01 0.0000E+00
0.1012E+00 0.0000E+00
0.1334E+00 0.0000E+00
0.1695E+00 0.0000E+00
0.2076E+00 0.0000E+00
0.2451E+00 0.0000E+00
0.2788E+00 0.0000E+00
0.3057E+00 0.0000E+00
0.3231E+00 0.0000E+00
0.3291E+00 0.0000E+00
0.3231E+00 0.0000E+00
0.3057E+00 0.0000E+00

0.2788E+00 0.0000E+00
0.2451E+00 0.0000E+00
0.2076E+00 0.0000E+00
0.1695E+00 0.0000E+00
0.1334E+00 0.0000E+00
0.1012E+00 0.0000E+00
0.7401E-01 0.0000E+00
0.5216E-01 0.0000E+00
0.3542E-01 0.0000E+00
0.2319E-01 0.0000E+00
0.1463E-01 0.0000E+00
0.8898E-02 0.0000E+00
0.5216E-02 0.0000E+00
0.2946E-02 0.0000E+00
0.1604E-02 0.0000E+00
0.8420E-03 0.0000E+00
0.4259E-03 0.0000E+00
0.2076E-03 0.0000E+00
0.9757E-04 0.0000E+00
0.4419E-04 0.0000E+00
0.1929E-04 0.0000E+00
0.8115E-05 0.0000E+00
0.3291E-05 0.0000E+00
0.1286E-05 0.0000E+00
0.4845E-06 0.0000E+00
0.1759E-06 0.0000E+00
0.6156E-07 0.0000E+00
0.2076E-07 0.0000E+00
0.6750E-08 0.0000E+00
0.2115E-08 0.0000E+00
0.6387E-09 0.0000E+00

0.1859E-09 0.0000E+00
0.5216E-10 0.0000E+00
0.1410E-10 0.0000E+00
0.3675E-11 0.0000E+00
0.9232E-12 0.0000E+00
0.2235E-12 0.0000E+00
0.5216E-13 0.0000E+00
0.1173E-13 0.0000E+00
0.2543E-14 0.0000E+00
0.5312E-15 0.0000E+00
0.1070E-15 0.0000E+00
0.2076E-16 0.0000E+00
0.3884E-17 0.0000E+00
0.7003E-18 0.0000E+00
0.1217E-18 0.0000E+00
0.2038E-19 0.0000E+00
0.3291E-20 0.0000E+00
0.5120E-21 0.0000E+00
0.7679E-22 0.0000E+00
0.1110E-22 0.0000E+00
0.1546E-23 0.0000E+00
0.2076E-24 0.0000E+00
0.2687E-25 0.0000E+00
0.3352E-26 0.0000E+00
0.4030E-27 0.0000E+00
0.4670E-28 0.0000E+00
0.5216E-29 0.0000E+00
0.5614E-30 0.0000E+00
0.5825E-31 0.0000E+00
0.5825E-32 0.0000E+00
0.5614E-33 0.0000E+00

0.5216E-34 0.0000E+00

0.4670E-35 0.0000E+00

0.4030E-36 0.0000E+00

0.3352E-37 0.0000E+00

Reference

H. B. Schlegel, J. M. Millam, S. S. Iyengar, G. A. Voth, A. D. Daniels, G. E. Scuseria, and M. J. Frisch, *J. Chem. Phys.* 114 (2001)

S. S. Iyengar, G. A. Parker, D. J. Kouri, D. K. Hoffman, *J. Chem. Phys.* 110 (1999)

D. K. Hoffman, N. Nayer, O. A. Sharefeddin, D. J. Kouri, *J. Phys. Chem.* 95 (1991)

M. Tuckerman, B. J. Berne, G. J. Martyna, *J. Chem. Phys.* 97(3) (1992)

Quantum Wavepacket Atom-centered Density Matrix Propagation: An approach to study quantum dynamics in large systems, S. S. Iyengar, J. Jakowski, *J. Chem. Phys.* 122, 114105 (2005)

Victor Guallar, Benjamin F. Gherman, William H. Miller,* Stephen J. Lippard,* and Richard A. Friesner*